2011 8th International Multi-Conference on Systems, Signals & Devices

PERFORMANCE ANALYSIS OF A WIND ENERGY CONVERSION SYSTEM BASED ON A DOUBLY-FED INDUCTION GENERATOR

Fatma HACHICHA, Lotfi KRICHEN

National Engineering School of Sfax, Advanced Control and Energy Management (ACEM)
BP 1173, 3038, Sfax, Tunisia

ABSTRACT

This paper is interested in the study of a wind energy conversion system (WECS) based on a doubly fed induction generator (DFIG) connected to the electric power network. The aim of this work is to compare the energy production unit performances by the use of two types of controllers. Classical PI and polynomial RST controllers are applied for the WECS control in terms of instruction tracking and robustness with respect to the wind fluctuation and the impact on the produced energy quality. A vector control with stator flux orientation of the DFIG is also presented.

Index Terms— Wind energy, DFIG, PI controller, RST controller.

1. INTRODUCTION

One of the most exploited among renewable energies is the wind power with an increasing growth rate all over the world. However, the wind device uses several physics phenomena (aerodynamic, mechanics, electric and thermal) and requires more researches to maintain energy effectiveness with a minimal system cost [1,2].

The use of the doubly fed induction machines was the subject of many investigation in research and especially in generator mode for the wind turbine [3,4]. It is important that the generator can function at variable speed but the presence of converters between the generator and the network harms the global efficiency of the installation. The DFIG proposes a good compromise between the variation speed range which it authorizes and the converters size compared to the machine nominal power. Several control strategies were established to control the power exchange between the machine and the network which is connected to [5-8].

Within this framework, we will present a comparative study between two types of regulators used for the control of the WECS at the level of the DFIG vector control and the connection to the network. Initially, a control with a PI regulator is carried out. This type of regulator is the most used for the control of many industrial system regulations because of the simplicity of its synthesis. Then the used regulator is a RST controller which concerns three polynomials. This regulator, whose synthesis is purely algebraic, is an algorithm more sophisticated based on placement theory of poles which exploits many numerical resources. A performance analysis will be established according to the obtained results using Matlab-Simulink.

2. DESCRIPTION OF THE STUDIED SYSTEM

As Fig.1 shows, the studied system comprises a variable speed wind turbine (VSWT) actuating a DFIG with a stator directly coupled to the electric network and a rotor connected through two pulse width modulation (PWM) converters, a DC bus and a RL filter. The presence of a converter between the rotor and the network allows the control of the power transfer between the stator and the network. Moreover, if the variation speed range is limited to ± 30% around synchronism, the converter can be dimensioned for only 30% of the machine nominal power [9]. The electric power can be not only produced from stator to the network but also from the rotor to the network for speeds higher than synchronism.

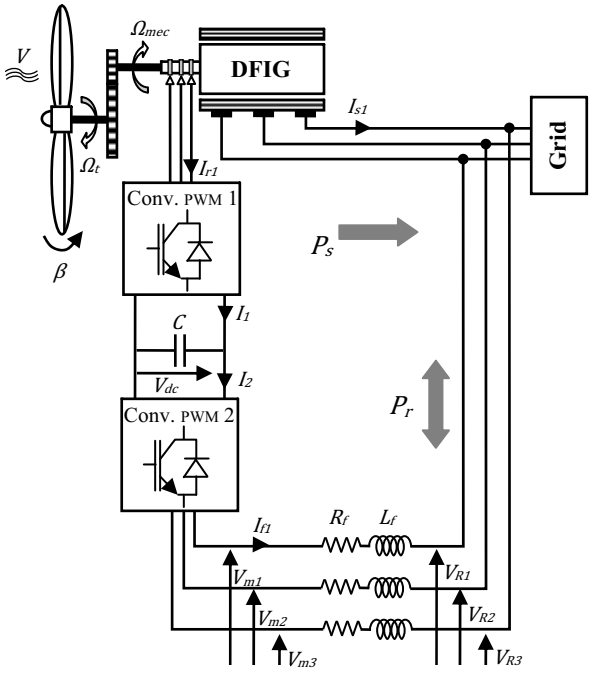

Figure 1. Wind energy conversion system structure.

978-1-4577-0411-6/11/$26.00 ©2011 IEEE

3. WECS MODELING

3.1. Wind turbine model

The behavior of the wind turbine can be simulated by determining the torque applied on its shaft.

The expression of the mechanical power extracted from the wind turbine is given by [10]:

$$P_w = \frac{1}{2}\rho\pi R^2 {V_w}^3 C_p(\lambda, \beta) \quad (1)$$

The power coefficient C_p depends on the rotor blades angle β and the tip speed ratio λ, with [11]:

$$\lambda = \frac{R\Omega}{V_w} \quad (2)$$

By dividing the mechanical power by the rotational speed, we obtain the turbine torque as:

$$T_m = \frac{P_w}{\Omega} \quad (3)$$

From the dynamics fundamental relation, we determine the turbine speed evolution as:

$$J\frac{d\Omega}{dt} = T_m - T_{em} - f\Omega \quad (4)$$

The diagram of the wind turbine model is shown in Fig.2.

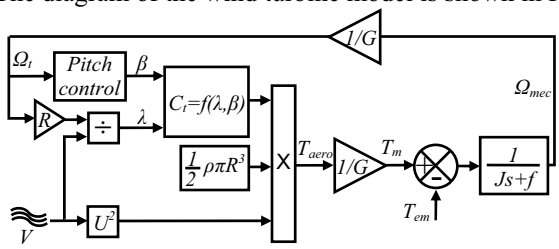

Figure 2. Wind turbine model.

3.2. DFIG model

The DFIG model is described in the Park reference frame by the following equations [7]:

$$\frac{d\Phi_{sd}}{dt} = -R_{sl}I_{sd} + \omega_s\Phi_{sq} + V_{Rd} \quad (5)$$

$$\frac{d\Phi_{sq}}{dt} = -R_{sl}I_{sq} - \omega_s\Phi_{sd} + V_{Rq} \quad (6)$$

$$\frac{d\Phi_{rd}}{dt} = -R_rI_{rd} + \omega_r\Phi_{rq} + V_{rd} \quad (7)$$

$$\frac{d\Phi_{rq}}{dt} = -R_rI_{rq} - \omega_r\Phi_{rd} + V_{rq} \quad (8)$$

Relations between fluxes and currents give the following magnetic equations:

$$\Phi_{sd} = L_{sl}.I_{sd} + M.I_{rd} \quad (9)$$

$$\Phi_{sq} = L_{sl}.I_{sq} + M.I_{rq} \quad (10)$$

$$\Phi_{rd} = L_r.I_{rd} + M.I_{sd} \quad (11)$$

$$\Phi_{rq} = L_r.I_{rq} + M.I_{sq} \quad (12)$$

The rotor and the stator angular speed are linked by the following relation:

$$\omega_r = (\omega_s - p\omega_{mec}) \quad (13)$$

The vector control strategy applied to the DFIG consists on making the stator flux in quadrature with the q-axis of the Park reference frame, therefore $\Phi_s = \Phi_{sd}$ and $\Phi_{sq} = 0$

Then equations from (5) to (8) can be simplified as:

$$\frac{d\Phi_{sd}}{dt} = -R_{sl}I_{sd} + V_{Rd} \quad (14)$$

$$V_{Rq} = R_{sl}I_{sq} + \omega_s\Phi_{sd} \quad (15)$$

$$\frac{d\Phi_{rd}}{dt} = -R_rI_{rd} + \omega_r\Phi_{rq} + V_{rd} \quad (16)$$

$$\frac{d\Phi_{rq}}{dt} = -R_rI_{rq} - \omega_r\Phi_{rd} + V_{rq} \quad (17)$$

From magnetic equations, stator currents are written as :

$$I_{sq} = -\frac{M}{L_{sl}}I_{rq} \quad (18)$$

$$I_{sd} = \frac{\Phi_{sd} - MI_{rd}}{L_{sl}} \quad (19)$$

By replacing these currents in the rotor flux equations, we obtain:

$$\Phi_{rd} = \left(L_r - \frac{M^2}{L_{sl}}\right)I_{rd} + \frac{M}{L_{sl}}\Phi_{sd} \quad (20)$$

By introducing the leakage coefficient σ with:

$$\sigma = 1 - \frac{M^2}{L_{sl}L_r} \quad (21)$$

We obtain:

$$\Phi_{rd} = L_r\sigma I_{rd} + \frac{M}{L_{sl}}\Phi_{sd} \quad (22)$$

$$\Phi_{rq} = L_r\sigma I_{rq} \quad (23)$$

By replacing equations (22) and (23) in (16) and (17), we obtain:

$$V_{rd} = R_rI_{rd} + L_r\sigma\frac{dI_{rd}}{dt} + \frac{M}{L_{sl}}\frac{d\Phi_{sd}}{dt} - \omega_rL_r\sigma I_{rq} \quad (24)$$

$$V_{rq} = R_rI_{rq} + L_r\sigma\frac{dI_{rq}}{dt} + \omega_rL_r\sigma I_{rd} + \frac{M}{L_{sl}}\omega_r\Phi_{sd} \quad (25)$$

Equations (20) and (21) constitute the basis of the DFIG regulation. Fig. 3 shows the control structure applied to the rotor side converter to regulate rotor currents, with $C_{(s)}$ is a PI or RST controller.

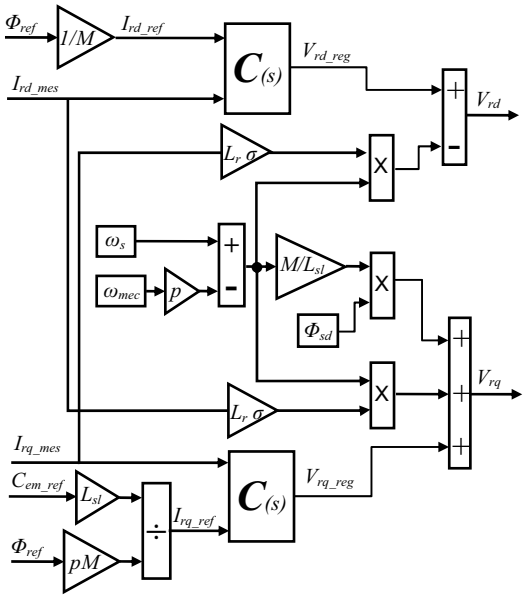

Figure 3. DFIG vector control strategy

3.3. Power converter model

The concept of instantaneous average value has been used to model converters. For each power switch, a switching function represent the ideal commutation orders and takes the values 1 when the switch is closed (on) and 0 when it is opened (off):

$$f_{ij} \in \{0,1\},$$

$$with \begin{cases} i \in \{1,2,3\} \ no.\ of\ the\ leg \\ j \in \{1,2\} \ no.\ of\ the\ switch\ in\ the\ leg \end{cases}$$

Considering an ideal power switches, the switches of a same leg are in complementary states:

$$f_{i1} + f_{i2} = 1$$

For both PWM converters of Fig. 1, modulation functions can be defined from the switching functions as:

$$m_{conv} = \begin{bmatrix} m_{conv13} \\ m_{conv23} \end{bmatrix} = \begin{bmatrix} 1 & 0 & -1 \\ 0 & 1 & -1 \end{bmatrix} \begin{bmatrix} f_{11} \\ f_{21} \\ f_{31} \end{bmatrix}_{conv}$$

3.4. Filter model

The connection of the rotor to the electric network is carried out via an R_fL_f filter, which has the role to attenuate harmonics frequency coming from power converter commutations.

Equations of the filter connected to the grid in the Park reference frame are expressed by [8]:

$$V_{md} = R_f I_{fd} + L_f \frac{dI_{fd}}{dt} - \omega_s L_f I_{fq} + V_{Rd} \quad (26)$$

$$V_{mq} = R_r I_{rq} + L_f \frac{dI_{fq}}{dt} + \omega_s L_f I_{fd} + V_{Rq} \quad (27)$$

A vector control of the filter currents has been carried out using a referential synchronized to the grid voltages.

The Fig.4 shows a bloc diagram of the control strategy applied to the grid side converter to control filter currents.

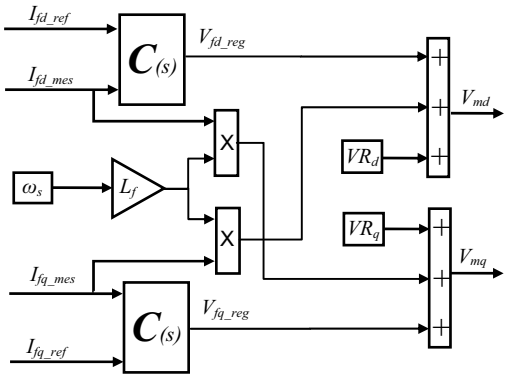

Figure 4. Grid side converter control.

4. CONTROLLER SYNTHESIS

4.1. PI controller

A PI controller has the following form:

$$C(s) = K_p + \frac{K_i}{s} \quad (28)$$

For a transfer function *H(s)*, with:

$$H(s) = \frac{Y_o}{Y_i} = \frac{1}{a + b.s} \quad (29)$$

We obtain the closed-loop system represented in Fig….

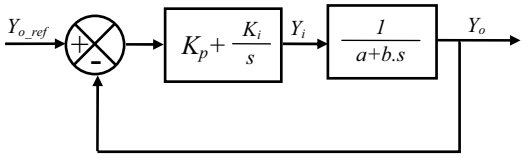

Figure 5. PI controller system

The closed-loop transfer-function of the controlled system is written as:

$$CLTF = \frac{K_p s + K_i}{K_i + (K_p + a)s + b.s^2} \quad (30)$$

Which can be expressed as follow:

$$CLTF = \frac{1 + \frac{K_p}{K_i} s}{1 + \frac{K_p + a}{K_i} s + \frac{b}{K_i} s^2} \quad (31)$$

By identifying the CLTF denominator with a second order polynomial P:

$$P = 1 + \frac{2\xi}{\omega_n} s + \frac{1}{{\omega_n}^2} s^2 \quad (32)$$

with ξ is the damping ratio and $\omega_n$is the resonance.
We obtain: $K_i = b.{\omega_n}^2$ and $K_p = 2\xi b\omega_n - a$
By applying Laplace transformer to equations (24) and (25), the transfer function becomes:

$$\frac{I_{rd}(s)}{V_{rd}(s)} = \frac{I_{rq}(s)}{V_{rq}(s)} = \frac{1}{R_r + sL_r\sigma} \quad (33)$$

Then, for the DFIG vector control, controller parameters are as follow:

$K_i = L_r\sigma{\omega_n}^2$ and $K_p = 2\xi L_r\sigma\omega_n - R_r$

By applying Laplace transformer to equations (26) and (27), the transfer function becomes:

$$\frac{I_{fd}(s)}{V_{md}(s)} = \frac{I_{fq}(s)}{V_{mq}(s)} = \frac{1}{R_f + sL_f} \quad (34)$$

Then, for filter currents control, controller parameters are as follow:

$K_i = L_f{\omega_n}^2$ and $K_p = 2\xi L_f\omega_n - R_f$

4.2. RST controller

The closed-loop system of the RST controller is given by the following bloc diagram:

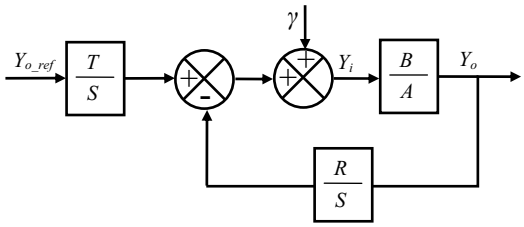

Figure 6. RST controller system

In our system, terms A and B are expressed by:
$A = R_r + sL_r\sigma$, $B = 1$; for the DFIG
$A = R_f + sL_f$, $B = 1$; for the filter
In general, $A = a + s.b$, $B = 1$;

RST controller is based on the pole placement theory which consists in specifying an arbitrary stability polynomial *D(s)* and calculate *S(s)* and *R(s)* according to the Bezout equation:

$$D = AS + BR \quad (35)$$

with deg(D)= deg(A)+ deg(S).

For our model, we obtain:

$$A = a_1 s + a_0 \quad (36)$$

$$B = b_0 \quad (37)$$

$$D = d_3 s^3 + d_2 s^2 + d_1 s + d_0 \quad (38)$$

$$R = r_1 s + r_0 \quad (39)$$

$$S = s_2 s^2 + s_1 s + s_0 \quad (40)$$

According to the robust pole placement strategy, the polynomial D is written as:

$$D = \left(s - \frac{1}{T_C}\right)\left(s - \frac{1}{T_f}\right)^2 \quad (41)$$

with T_c is the control horizon and T_f is the filtering horizon.

To accelerate the system, we adopt the following conditions:

$$T_C = \frac{b}{5a} \quad and \quad T_f = \frac{1}{3}\frac{b}{5a} \quad (42)$$

Then, polynomial D is written as:

$$D = \left(s + 5\frac{a}{b}\right)\left(s + \frac{15a}{b}\right)^2 \quad (43)$$

By identifying equations (38) and (43), we find coefficients of polynomial *D* which are linked to coefficients of *R* and *S* by the Sylvester matrix [8]. Thus, we can determine RST controller parameters as follow:

$$d_3 = a_1 s_2 \ \rightarrow \ s_2 = \frac{d_3}{a_1} \quad (44)$$

$$d_2 = a_1 s_1 \ \rightarrow \ s_1 = \frac{d_2}{a_1} \quad (45)$$

$$d_1 = a_0 s_1 + b_0 r_1 \ \rightarrow \ r_1 = \frac{d_1 - a_0 s_1}{b_0} \quad (46)$$

$$d_0 = b_0 r_0 \ \rightarrow \ r_0 = \frac{d_0}{b_0} \quad (47)$$

$$T = r_0 \quad (48)$$

5. PERFORMANCE ANALYSIS

Simulation of the WECS has been realized using Matlab-Simulink. The study consists in applying, at first, a PI controller to the rotor side converter for the DFIG vector control and also to the grid side converter to control filter currents. Then, the obtained results are compared to those coming from applying an RST controller.

We have applied to the wind turbine a variable wind between 7 and 14 m/s, as represented in Figure 7.
We observe that mechanical speed follows the wind profile as Figure 8 shows with a limitation to +30% of the nominal speed due to the pitch angle variation as represented in Figure 9. This limitation authorizes a dimensioning of the power converters to the third of the nominal power; this choice allows minimizing installation cost.

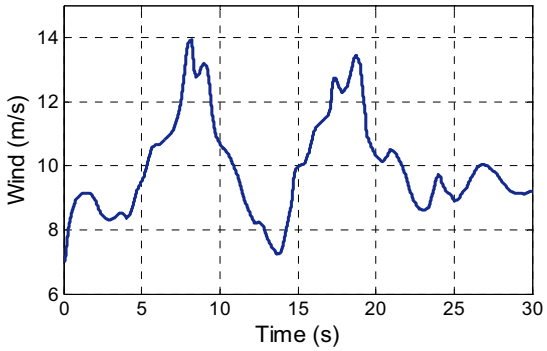

Figure 7. Wind speed.

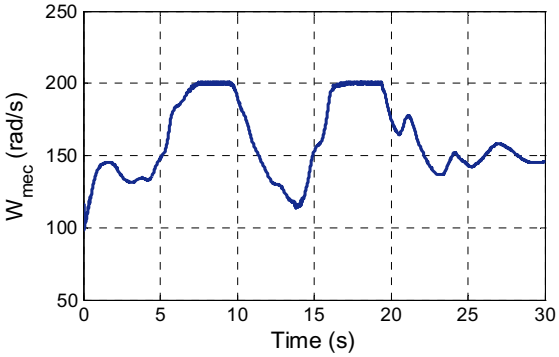

Figure 8. Rotational speed.

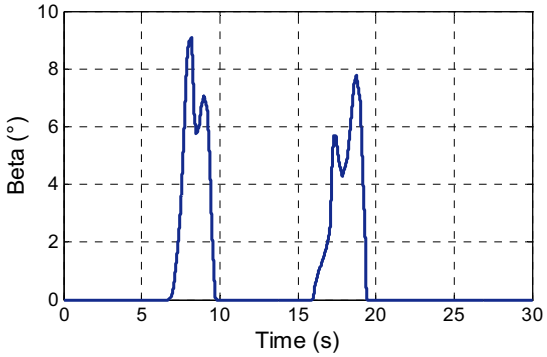

Figure 9. Blade angle.

Figure 10 shows the aerodynamic power generated by the wind turbine and the rotor power which is positive in hyposynchrone mode ($w_r < w_s$; the rotor absorbs power from the network) and negative in hypersynchrone mode ($w_r > w_s$; the rotor provides power to the network). The stator power is limited to the nominal value and the excess of power is transferred by the rotor. The power injected to the network corresponds to the sum of the stator and rotor powers.

From these figures, we observe that powers of the system controlled with an RST regulator present less disturbances than that of the system controlled with PI regulator especially in limits operation area what influences the produced energy quality and this translated by the robustness of the RST controller compared to PI.

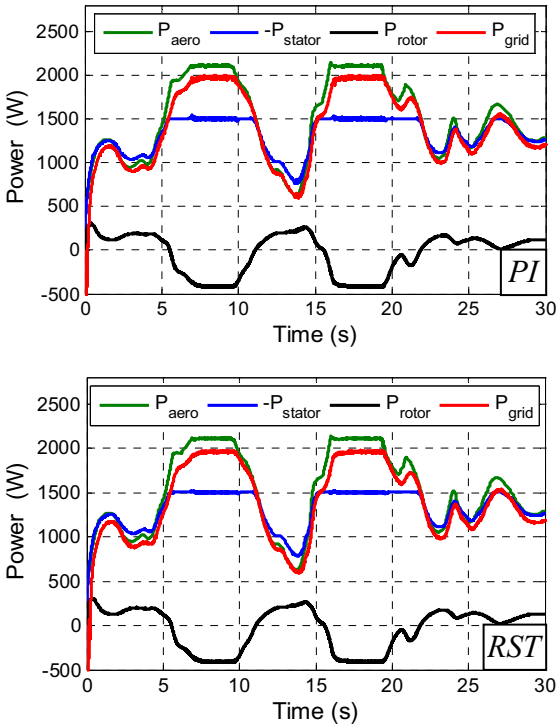

Figure 10. Power assessment.

Rotor currents and filter currents in the Park reference frame are represented in Figure 11 and Figure 12. These two figures show a good instructions tracking for the two types of regulators but currents are less disturbed with RST regulators.

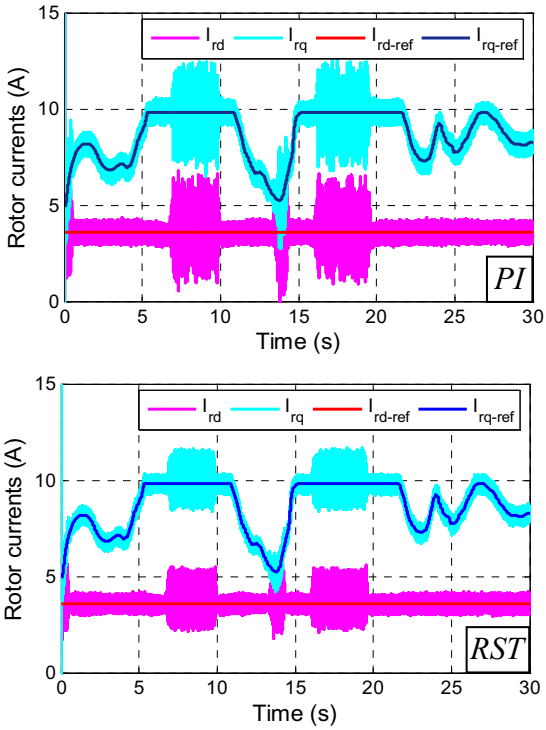

Figure 11. Rotor currents.

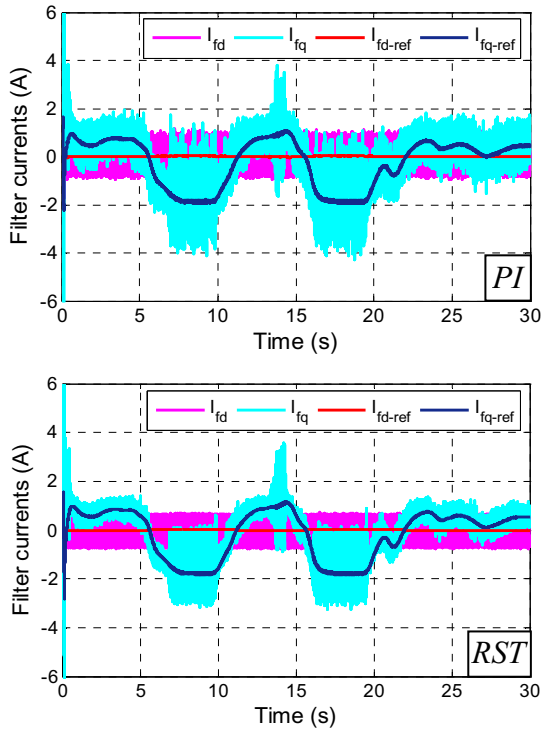

Figure 12. Filter currents.

The control of the filter currents is carried out by the grid side converter in order to maintain a constant DC bus voltage and equal to the reference value of 400V. This voltage is represented in Figure 13 and it is noticed that there is a small difference between the two controllers.

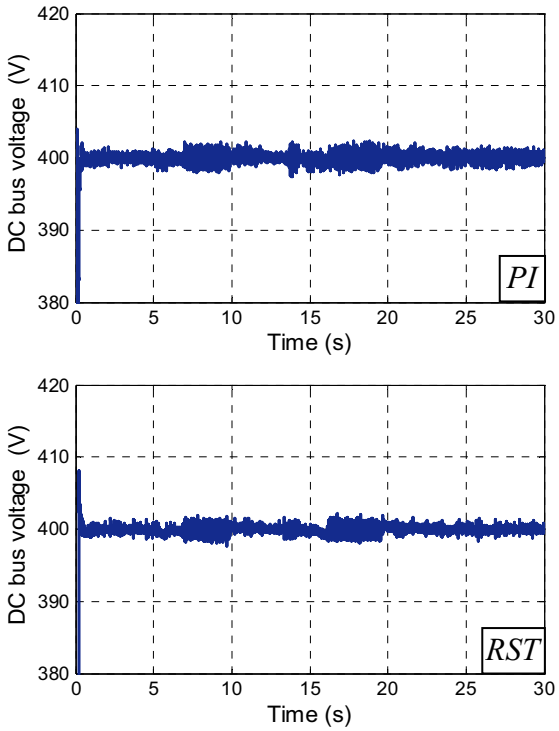

Figure 13. DC bus voltage.

6. CONCLUSION

We have presented in this paper, a modeling and a control of a WECS based on DFIG with a stator directly connected to the electrical network and a rotor also connected by the way of two power converters. The rotor side converter has been used to control the DFIG power transfer and the grid side converter has been controlled to maintain a DC bus constant voltage. This control has been carried out using PI and RST controller. Simulation results show that the use of RST controller is more interesting to have better energy quality; the only difficulty with this type of regulator is parameters adjustment.

7. REFERENCES

[1] J.Wen, Y.Zheng, F.Donghan, A review on reliability assessment for wind power, J. Renewable and Sustainable Energy Reviews 13 (9) (2009) 2485–2494.

[2] M.Hoogwijk, B.de Vries, W.Turkenburg, Assessment of the global and regional geographical, technical and economic potential of onshore wind energy, J. Energy Economics 26 (5) (2004) 889– 919.

[3] A. Tapia, G. Tapia, J.X. Ostolaza, J.R. Saenz, Modeling control of a wind turbine driven doubly fed induction generator, IEEE Trans. Energy Convers. 18 (2) (2003) 194–204.

[4] S. Muller, M. Deicke, W. Rik, De Doncker, ‘‘Doubly fed induction generator systems for wind turbines’’, IEEE Ind. Appl. Magazine 8 (3) (May/June 2002) 26–33.

[5] Lie XuCartwright P. Direct active and reactive power control of DFIG for wind energy generation. IEEE Transactions on Energy Conversion Sept. 2006;21(3):750–758.

[6] Hee-Sang Ko, Gi-Gab Yoon, Nam-Ho Kyung,Won-Pyo Hong, Modeling and control of DFIG-based variable-speed wind-turbine; Electric Power Systems Research 78 (2008) 1841–1849

[7] B. Boukhezzar , H. Siguerdidjane, Nonlinear control with wind estimation of a DFIG variable speed wind turbine for power capture optimization; Energy Conversion and Management 50 (2009) 885–892

[8] F. Poitiers, T. Bouaouiche, M. Machmoum ; Advanced control of a doubly-fed induction generator for wind energy conversion, Electric Power Systems Research 79 (2009) 1085–1096

[9] R. Datta, V.T. Ranganathan, Variable-speed wind power generation using doubly fed wound rotor induction machine – a comparison with alternative schemes, IEEE Transactions on Energy Conversion 17 (3) (2002) 414–421.

[10] E. Muljadi, C.P. Butterfield, Pitch-controlled variable-speed wind turbine generation, IEEE Trans. Industry Appl. 37 (1) (2001) 240–246.

[11] J.G. Slootweg, S.W. De Haan, H. Polinder, W.L. Kling, General model for representing variable speed wind turbines in power system dynamics simulations, IEEE Trans Power Syst 18 (1) (2003) 144–151.